

Experimental and Theoretical Investigation of Multiphase Flow in Fractured Media

E. Rangel-German, S. Akin and L. Castanier
Petroleum Engineering Department, Stanford University

ABSTRACT

A laboratory flow apparatus was built to obtain data on water-air displacements in horizontal single-fractured block systems. For this purpose, two configurations have been used: a two matrix-block system with a 1mm spacer between the blocks, and a two matrix-block system with no spacer. During the experiments, porosity and saturation calculations along the cores have been made utilizing an X-ray Computerized Tomography (CT) scanner. Saturation images were reconstructed in 3-D to observe better matrix-fracture interactions. Differences in fluid saturations and relative permeabilities caused by changes in fracture width have also been analyzed. The fracture system without a spacer showed a more stable front and faster breakthrough than the other. However, the final water saturation was higher in the wide fracture system, thus showing that capillary pressure in the narrow fracture has more effect on recovery. Simulations of the experiments were made using a commercial reservoir simulator (Eclipse). Fracture relative permeability and capillary pressure curves were obtained by history matching the experiments. Sensitivity analysis of parameters such as fracture relative permeability, capillary pressure in the fracture, and fracture width were also conducted. The results showed that the assumption of fracture relative permeability equal to phase saturation is incorrect. Moreover, larger flow resistance in the fractures was observed by comparing the experiments with numerical simulation work. We found that the processes are both capillary and viscous dominated.

INTRODUCTION

Fractured porous media are usually comprised of two systems: a matrix system that contains most of the fluid storage, and a fracture system where fluids can flow more easily. Under this assumption, flow equations are written assuming that reservoir behavior is dominated by the transfer of fluid from the matrix to the high conductivity fractures, which are also often entirely responsible for flow between blocks and flow to wells.

Any representation of the material balance equation that describes the flow through fractured porous media will assume the knowledge of both rock and fluids properties, capillary pressure and relative permeabilities. Any of these parameters can be obtained for the matrix by laboratory work, but not for the properties for the fractures. To obtain more data on parameters such as fracture capillary pressure, fracture relative permeabilities and/or saturation distributions, further experimental work is necessary. Therefore, the purpose of this study is to investigate this problem both experimentally and by numerical simulation.

Previous experiments can be grouped into several broad categories: 1) imbibition dominated experiments, 2) gravity dominated experiments, and 3) flow in a single fracture experiments, which are mostly studied in geothermal and hazardous waste disposal problems, where the main topic is the understanding of flow with no or little matrix interaction in an attempt to obtain better fracture relative permeability data in more realistic fractures (Hughes, 1995).

In general, several authors (Kazemi and Merrill (1979), Beckner (1990), Gilman et al. (1994)) have assumed that fracture capillary pressures are negligible. Others have shown experimentally that capillary continuity becomes important when gravity provides a driving force (Horie et al. (1988), Firoozabadi and Hauge (1990), Labastie (1990), Firoozabadi and Markeset (1992)). Kazemi (1990) states his belief that capillary continuity is prevalent in the vertical direction and has suggested that, to reduce the number of equations to solve, fractured reservoir simulations should use the dual permeability formulation for the z direction and the dual porosity formulation for the x and y directions.

For this work, detailed measurements of pressure, rate, and saturation distribution were performed, and attempts to measure phase distribution inside the fracture were also made using a (CT) scanner. This research resulted in a much better understanding of the physical processes that occur when two or three phases flow in a fractured system, compared to previous reported studies (Guzman and Aziz (1993), Hughes (1995)). Our first step was constructing an experimental apparatus capable of reproducing the results obtained by that by Hughes(1995). Thus, we conducted similar experiments using two of the core holders developed by him in order to verify that this new experiment gives consistent results. Once the apparatus was tested, we conducted water-air flow experiments using an 8% NaBr brine solution as the wetting phase. Differences in fluid saturations and relative permeabilities caused by changes in fracture width were also analyzed.

Simulations of the experiments using a commercial reservoir simulator were performed. Fracture relative permeability and capillary pressure curves were obtained by history matching the experiments qualitatively. A sensitivity analysis of parameters such as fracture relative permeability, capillary pressure in the fracture, and fracture width was also made.

EXPERIMENTAL DESIGN AND PROCEDURE

Two Boise sandstone cores that are rectangular in shape were used. Due to the rectangular shape and the desire to measure in-situ saturations through the use of the CT scanner, conventional core holders could not be used. A core holder similar to the one designed by Guzman and Aziz (1993) later developed by Hughes (1995) was used. It consists of an epoxy resin surrounding the core as well as plexiglas end plates and a piece of 3/8 inch Viton acting as a gasket between the core and the plexiglas end plates as shown in Figure 1.

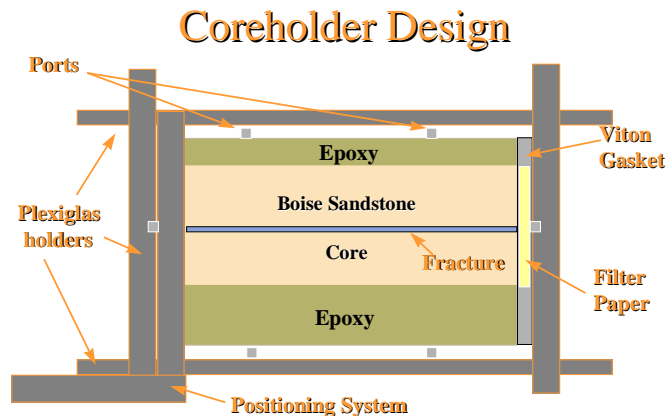


Figure 1. The Core Holder.

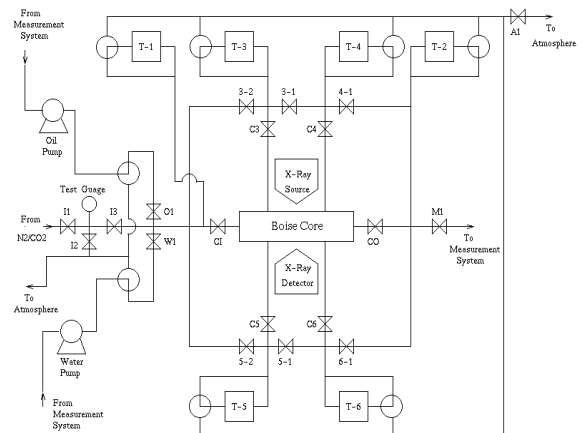


Figure 2. Flow System (After Hughes, 1995.)

The flow system shown in Figure 2 allows fluids to be directed to any port or combination of ports in the experiment such that 1)It can be directed to calibrate the pressure transducers, 2)It can be used to inject from one end and to produce from the opposite end, 3) It can be used to inject into one or more of the ports on the top and bottom of the core holder, or 4) To bypass the core holder completely. It also consists of two pumps that inject 0.01 to 9.99 cm³/min in 0.01 increments. Plumbing downstream of the pumps allows mixing of the fluids being discharged by each pump. This setup allows injection pressure to be monitored with a test gauge and recirculation to measure pump output rates. An 8% NaBr doped water was used as the water phase, since adding salts to water increases water density and allows higher resolution images from the CT Scanner.

The first core used had a fracture with no spacer in between the blocks. The total travel distance of the positioning system (accuracy \pm 0.01 mm) was then 25.5 cm, resulting in 13 slices including those two located at the pressure ports (fourth and eleventh, for the first experiment; and fourth and tenth, for the second one.) The second experiment was done using a coreholder that contained a similar system with two Boise sandstone blocks with a 1 mm thick fracture in between. Figure 3 shows the CT scan locations.

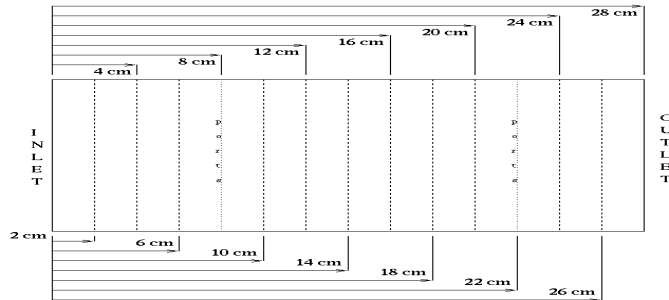


Figure 3. CT Scan Locations.

The first step of all experiments was to scan the dry core for reference dry images that are used to calculate the porosity and saturation distribution along the cores. The second step was to evaluate how water imbibed into an unsaturated core. Starting with a flow rate of 2 cm³/min, CT images of the core were taken every 5 minutes until the first 20 minutes of water injection (0.15 PV). After this, images were taken at regular intervals. Following that the top and bottom ports were opened to allow the core to the maximum water saturation. Common to all time steps, we tried to take images up to one location ahead of the water front. After 5 hours (2.25 PV) of water injection, the flow rate was dropped to 0.5 cm³/min and we injected water for 14 more hours to reach steady state. After 8.55 PV of water injected, reference 100% water saturated images were taken at the same locations. Two sets of CT slices were taken to find a possible change in CT numbers. Negligible changes in CT numbers were observed. Table 1 summarizes the flow rates used. The same experimental procedure was followed.

Table 1. Rates and Timing for the Core with Thin Fracture.

Fluid Injected	Time [hr.]	Flow Rate [cm ³ /min]	Ports
Water	0.0 - 4.0	2.0	Top and bottom closed, lateral open.
Water	4.0 - 5.0	2.0	Top and bottom open, lateral closed.
Water	5.0 - 19.8	0.5	Top and bottom open, lateral closed.
Water	19.8 - 23.0	2.0	Top and bottom closed, lateral open..

DATA ANALYSIS

Using the CT numbers obtained from the experiments, porosity and saturation distribution along the core were determined. The most common way to calculate porosity from CT Scanner images is by using the following expression (Withjack, 1988):

$$\phi = \frac{CT_{cw} - CT_{cd}}{CT_w - CT_a} \quad (1)$$

where CT_{cw} is the CT number for a 100% water saturated core at a matrix location, CT_{cd} is the CT number for a dry core at a matrix location, CT_w is the CT number for water, and CT_a is the CT number for air. The CT number for water (8% NaBr solution) is around 360, while the CT number for air is -1000. The water saturations were also calculated from the CT images. The following equation shows the way to evaluate water saturation for the water displacing air case.

$$S_w = \frac{CT_{aw} - CT_{cd}}{CT_{cw} - CT_{cd}} \quad (2)$$

RESULTS

First, we computed the values of porosity using Equation 1 at each location indicated in Figure 3. The porosity images for both systems are shown in Figure 4, where the values below each square correspond to the mean and the standard deviation, respectively, of the porosity values obtained from CT numbers. This step was essential for both experiments because from these images and their corresponding values we differentiated the regions with higher or lower porosity. The range of values are shown in the color bar in the right hand side in Figure 4. There, we can also see that the system with the thin fracture has a little higher porosity than the system with the wide fracture, especially in the top block, where values up to 0.13 were observed. We found that the average value for porosity calculated from the scans was 14.5% for the wide fracture system, which matches with the average value 14.35% reported by Hughes (1995).

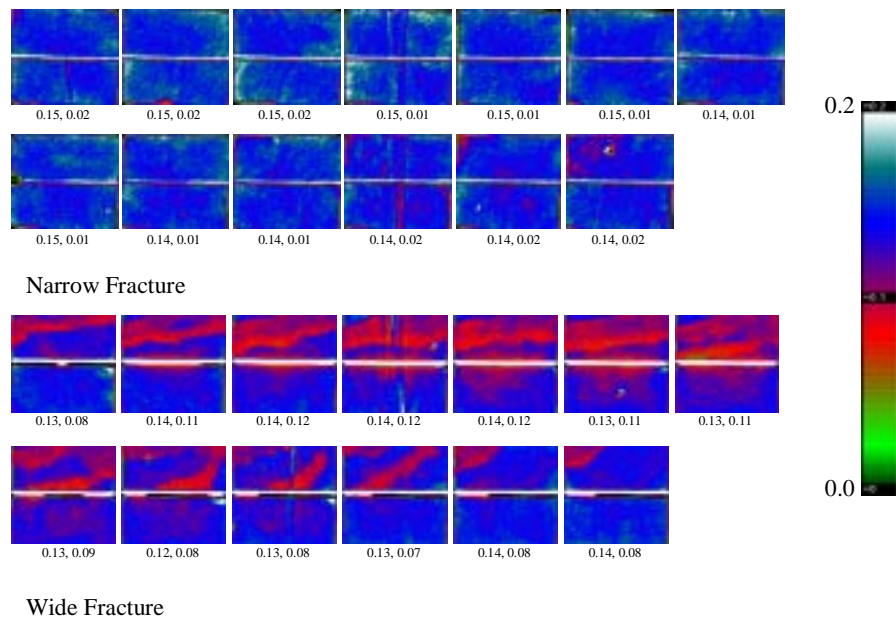


Figure 4. Porosity Distribution for the experimental system.

Following the aforementioned procedure, and the flow rates, times and injection/production conditions shown in Table 1, several sets of images like the one shown in Figure 5 corresponding to 1.5 hours of water injection (0.67 PV) were obtained. Similar to the porosity images, each square corresponds to water saturation values obtained at one location. The pair of values presented below each square corresponds to the mean and standard deviation of the top, bottom, and both blocks, respectively. The color bar on the right hand side shows the range of water saturation values. Different profiles, corresponding to different pore volumes of water injected were plotted. The profiles are more or less stable and they appear to be quasi one dimensional.

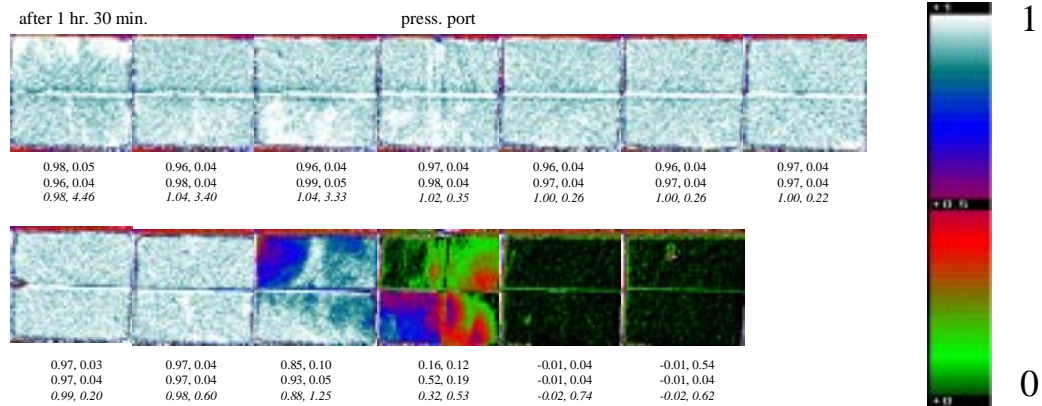


Figure 5. CT Saturation images for the Thin Fracture System after 1hr 30 min of Water injection.

The same procedure was followed for the wide fracture system and CT saturations were obtained. Figure 6 gives water saturation distribution at 0.67 PV of water injected. Different profiles, corresponding to different pore volumes of water injected were also plotted. The profiles are less stable than those for the thin fracture system as observed from the 8th through 12th slices. We observed similar profiles for all times (i.e. piston-like movement in thin fracture system, and unstable front in wide fracture system.)

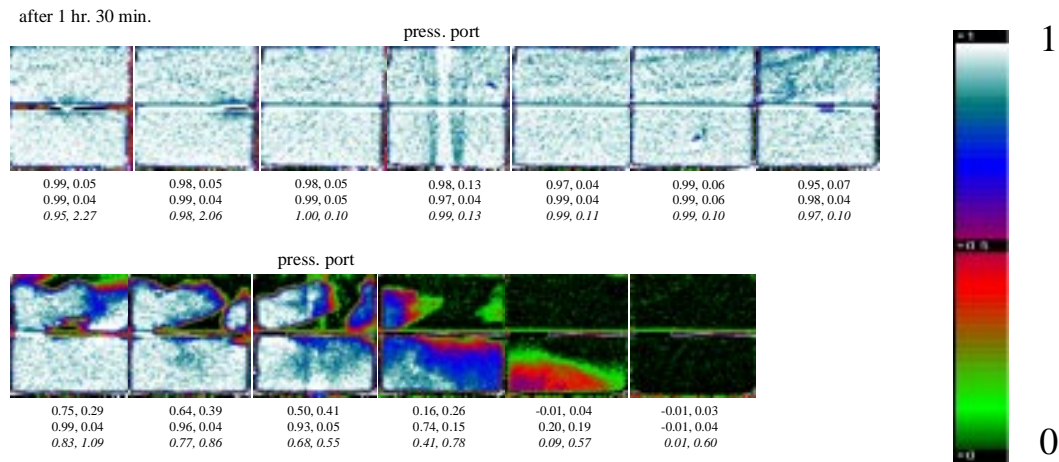


Figure 6. CT Saturation images for the Fracture System after 1hr 30 min of Water injection.

In order to have a better understanding of the processes and the differences between the flow patterns for different fracture widths, three dimensional (3-D) reconstruction of several sets of images were computed. These 3-D images show more clearly how the fluids actually flow through fractured porous media as shown in Figure 7. These reconstructions show water saturations greater than 50%. There, we can see how the water front for the wider fracture system goes almost at the same speed as the water front for the thinner fracture system does for the same time. For instance, one can see that after 1.5 hours of water injection, the water front in the thin fracture system seems to be ahead of the front for the wide fracture system; however, after two hours of water injection water has filled up both systems.

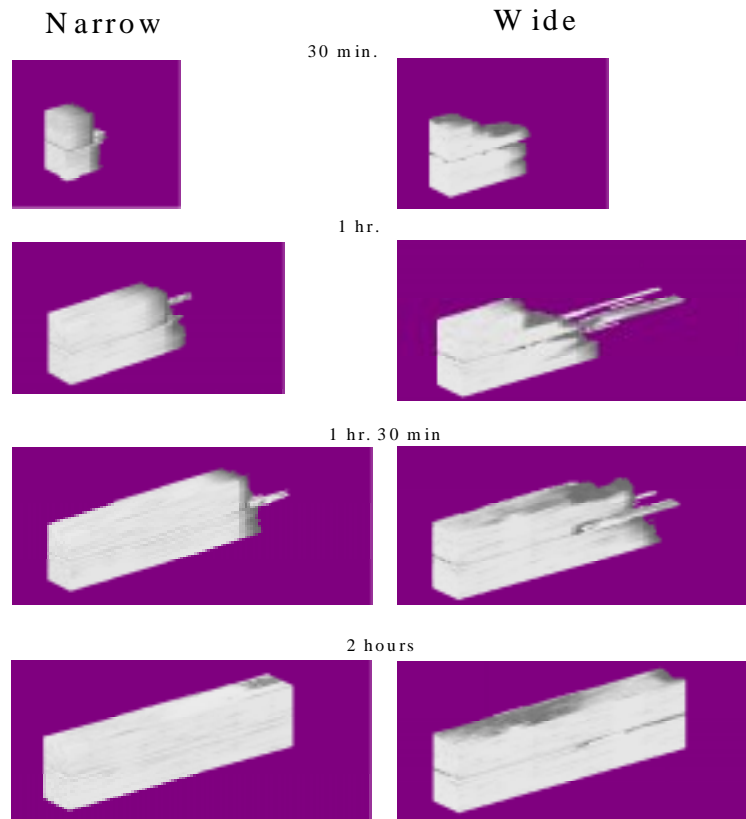


Figure 7. 3-D Reconstruction for both systems for $S_w \geq 0.5$.

It can be observed that for the thin fracture system the front is stable. The flow from the fracture to the matrix is clearly visible. That is to say, capillary continuity is maintained between the fracture and the matrix. However, for the wide fracture system the imbibition forces are not that strong and the front is not piston like. We also observed faster breakthrough times for the wide fracture.

NUMERICAL SIMULATION WORK

Simulations of the experiments using a commercial reservoir simulator have been completed. A cubic cartesian gridding proportional to the cores was designed in such a way that we had three different “boxes”. Two of them simulate the top and bottom blocks with matrix rock properties; i.e., matrix capillary pressure curves, matrix relative permeability curves, matrix absolute permeability, porosity, and the other set of blocks simulate the horizontal fracture with fracture properties; i.e., large absolute permeability, fracture capillary pressure curves, and fracture relative permeability curves. It was assumed that relative permeability and capillary pressure in the matrix are constant. We used the

curves presented by Persoff et. al. (1991). Fracture relative permeability and capillary pressure curves were obtained by history matching the experiments. Sensitivity analysis of parameters such as fracture relative permeability, capillary pressure in the fracture, and fracture width have been done. We considered each parameter independently.

First, we studied capillary pressure in the fracture under the assumption that it is a linear function of water saturation. Different cases for capillary pressure curves and relative permeability curves for the fracture are shown in Figure 8. It is important to note that for fracture relative permeability curves, the lower the slope of the straight line, the higher the resistance to flow through the fracture. Starting with a high capillary pressure in the fracture, we observed that the matrix front matched well, but the breakthrough time was faster compared to our experimental results. We decreased the slope of the straight line capillary pressure in the fracture up to a point in which the breakthrough time as well as the matrix front matched the experiments. For the sake of completeness, we also studied extreme cases that are often used in real practice such as very low and no capillary pressure in the fracture, although neither one resembled experimental data. The no capillary pressure case showed us that the blocks worked independently, so the capillary continuity that we had seen in the experiments did not occur in the numerical studies.

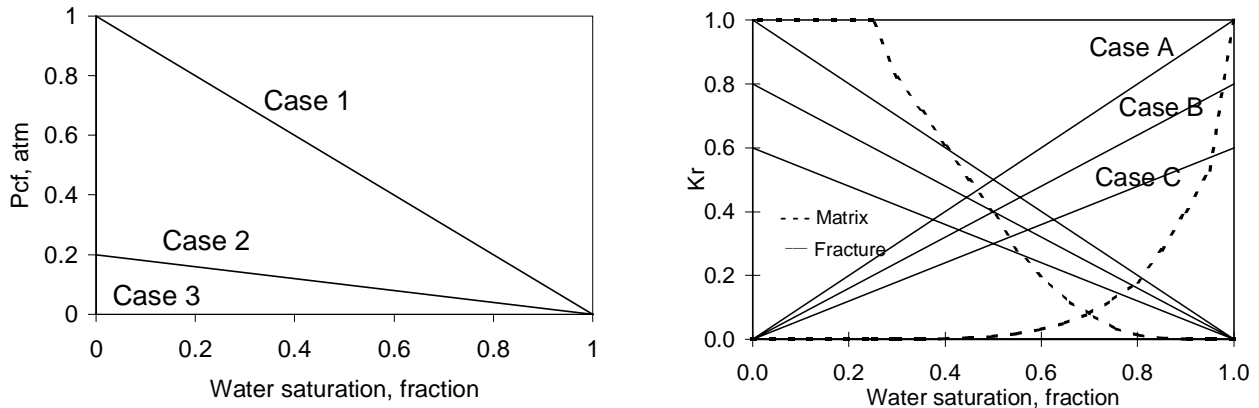


Figure 8. Different cases for capillary pressure curves and relative permeability curves for the fracture.

After obtaining the proper description of capillary pressure in the fracture, we continued by studying the effect of fracture relative permeability curves. The assumption of fracture relative permeability equal to phase saturation is often used in numerical simulation. This assumption suggests, no resistance, ideal flow of fluids in the fractures, such that inside the fracture the phases can move past each other without hindrance. However, if relative permeabilities with a slope less than 1.0 is used, the effective total mobility is reduced. Pan et. al. (1996) discussed that higher resistance in the fractures must be used, such as 0.8 and 0.6 slope straight lines instead. Our results show that the best matches are achieved when an 0.6 slope is used. This indicates that the presence of a small amount of one phase interferes significantly with the flow of the other phase.

In order to obtain the best match, we also examined the heterogeneities present in the systems, especially in the wide fracture system. So we ran different heterogeneous cases until we obtained better matches. We achieved this goal by assigning higher porosity (14%) to the bottom block and lower porosity (13%) to the top block. The results for this case are shown in Figure 9 which proves that, capillary pressure in the fracture can not be neglected and the heterogeneity must also be considered.

Similarly, we followed the same analysis for the system with no spacer in between the blocks. An interesting observation was that neither the capillary pressure in the fracture nor the relative permeability curves affected the results. That lead us to the conclusion that the fracture is so thin that there is almost perfect continuity, and it acts like a solid block. Figure 9 also shows the comparison of the experimental results with the numerical simulation results for the system with no spacer. The fracture system without a spacer showed a more stable front and faster breakthrough than the other, as we had seen in the experimental results.

CONCLUSIONS

The results of the combined experimental and the simulation study show:

1. Areas with lower permeability and porosity were identified and used in numerical simulations.
2. Thin fracture system showed more stable fronts and slower breakthrough compared to wide fracture systems.
3. Capillary pressure has more effect when the fractures are narrow.
4. Larger recoveries can be obtained when the fractures are wider.
5. Assuming zero capillary pressure in the fracture is incorrect.
6. X-type relative permeability curves can be used for fractured systems using high resistance through fractures.

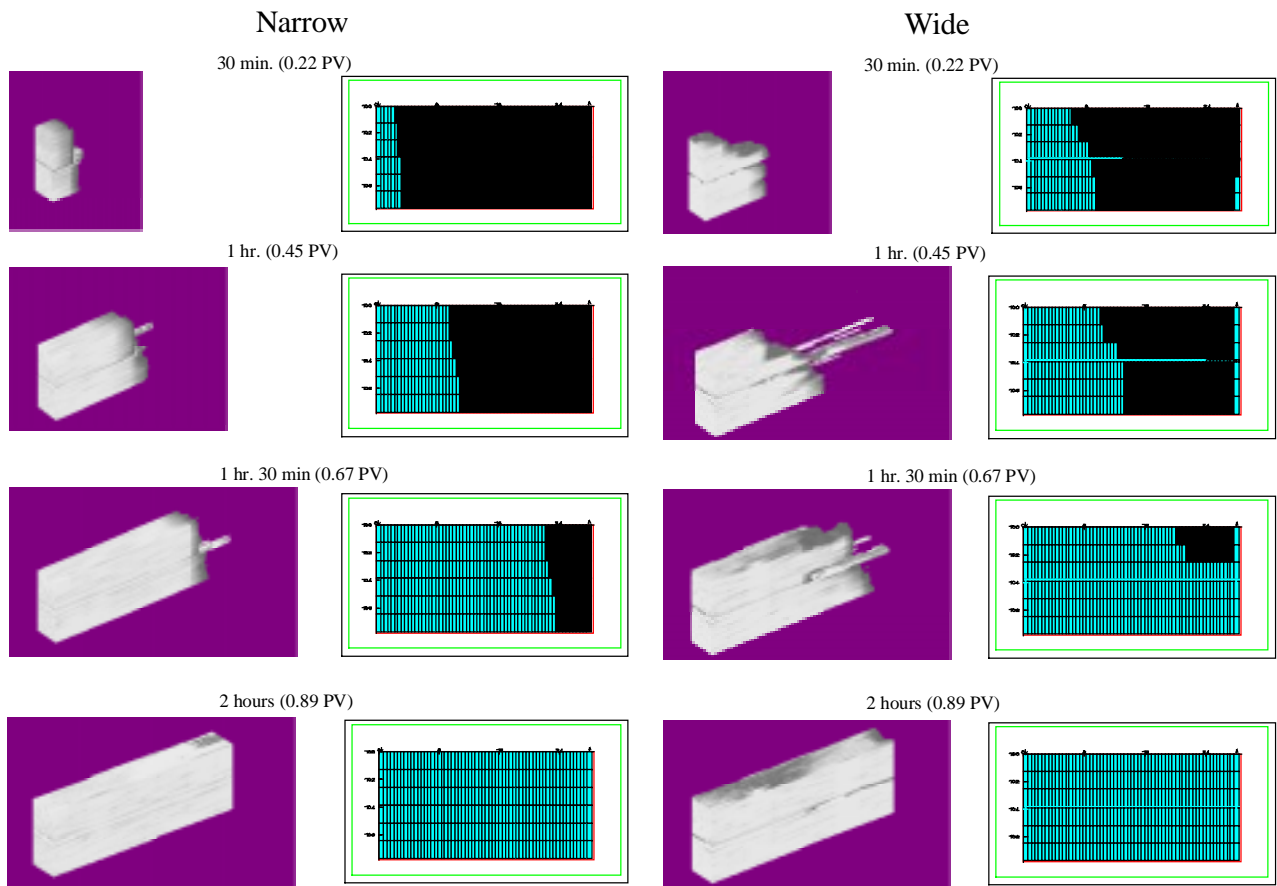


Figure 9. Comparison between experiments and simulations for narrow and wide fracture systems.

ACKNOWLEDGEMENTS

This work is supported by U.S. Department of Energy under contract No. DE-FG22-96BC14994, SUPRI-A Industrial Affiliates and Consejo Nacional de Ciencia y Tecnología (CONCACyT), México.

REFERENCES

- Beckner, B.L.: *Improved Modeling of Imbibition Matrix/Fracture Fluid Transfer in Double Porosity Simulators*, PhD dissertation, Stanford University (July 1990)
- Buckley, S.E. and Leverett, M.C.: "Mechanisms of Fluid Displacement in Sands," Transactions American Institute of Mining and Metallurgical Engineers, 146 (1942), 107-116.
- Eclipse 100 User's Manual, Intera Information Technology Limited, Oxfordshire, England, 1994.
- Firoozabadi, A. and Hauge, J.: "Capillary Pressure in Fractured Porous Media," JPT (June 1990) 784-791.
- Firoozabadi, A. and Markeset, T.: "An Experimental Study of Capillary and Gravity Crossflow in Fractured Porous Media," SPE 24918, presented at the 67th SPE Annual Technical Conference and Exhibition, Washington, D.C., October 4-7, 1992.
- Gilman, J.R., Bowzer, J.L. and Rothkopf, B.W.: "Application of Short-Radius Horizontal Boreholes in the Naturally Fractured Yates Field," SPE 28568, presented at the 69th SPE Annual Technical Conference and Exhibition, New Orleans, LA, September 25-28, 1994.
- Guzman, R.E. and Aziz, K.: *Design and Construction of an Experiment For Two-Phase Flow in Fractured Porous Media*, SUPRI TR-95, Stanford Petroleum Research Institute, Stanford, CA, (June 1993).
- Horie, T., Firoozabadi, A. and Ishimoto, K.: "Capillary Continuity in Fractured Reservoirs," SPE 18282, presented at the 63rd SPE Annual Technical Conference and Exhibition, Houston, TX, October 2-5, 1988.
- Hughes, R.G.: *CT Measurements of Two-Phase Flow in Fractured Porous Media*, Masters Report, Stanford University (December 1995).
- Kazemi, H. and Merrill, L.S.: "Numerical Simulation of Water Imbibition in Fractured Cores," SPEJ (June 1979) 175-182.
- Kazemi, H.: *Naturally Fractured Reservoirs*, Third International Forum on Reservoir Simulation, Baden, Austria (1990).
- Labastie, A.: "Capillary Continuity Between Blocks of a Fractured Reservoir," SPE 20515 presented at the 65th SPE Annual Technical Conference and Exhibition, New Orleans, LA, September 23-26, 1990.
- Pan, X. and Wong, R.C.: "Steady State Two-phase in a Smooth Parallel Fracture," presented at the 47th Annual Technical Meeting of The Petroleum Society in Calgary, Alberta, Canada, June 10-12, 1996.
- Persoff, P., Pruess, K., and Myer, L.: "Two-Phase Flow Visualization and Relative Permeability Measurement in Transparent Replicas of Rough-Walled Rock Fractures," Sixteenth Workshop on Geothermal Reservoir, Stanford University (January 1991).
- Withjack, E.M.: "Computed Tomography for Rock-Property Determination and Fluid-Flow Visualization", SPEFE (December, 1988) 696-704.